International Journal of Innovative Technology and Exploring Engineering (IJITEE)
ISSN: 2278-3075 (Online), Volume-8 Issue-11, September 2019

Numerical Simulation Of Hydrodynamic Cavitation In Centrifugal Pump

Micha Premkumar T, Sathish Babu R, Vinoth Kumar M, Hariram V, Seralathan S

Abstract*: The diffusion of computational fluid dynamics to analysis fluid flow is established thoroughly in pump manufacturing industries. It increases the flexibility in analyzing the various pump parameters under design and off-design condition. The key steps involved are the design calculation, computer aided model, Auto mesh using Turbo-gird tool of ANSYS©, computational fluid dynamics Analysis. This enable the pump engineer to analysis the given pump before actually fabricating the pump which reduce the wastage and downtime in correcting the underperforming turbine. Moreover, the performance of the pump under cavitating condition is analyzed numerically, it shows that the computational fluid dynamics tool is versatile in analyzing the performance of the pump at no time with high accuracy and help to expand the research and development in the pump industry. The experimental data of the similar pump is used as the key to validate the computational fluid dynamics code to improve the reliability of the computational fluid dynamics prediction. It is observed from the numerical simulation that the suction surface of the impeller led to separation and re-circulation at off-design condition (1.2 times of discharge) which in-turn influence the onset of cavitation at the leading edge of the blade.

Keywords: Computational fluid dynamics, turbomachine, cavitation, cross-flow, impeller.

I. INTRODUCTION

The prediction of the performance of the turbo-machine through Computational Fluid Dynamics (CFD) is the important tool to modernize the Pump Industries. Moreover, Design and Optimization of hydrodynamic performance of the pump is made easier through this tool. It can also predict the unfavourable occurrence in the like separation, recirculation and reverse flow during the off-design condition [1, 2]. The qualitative information about the interaction of secondary flow and the formation of the viscous sub-layer due to unfavourable pressure gradient is measured using this tool effectively. Moreover, all the above unfavourable incident in the impeller of the centrifugal pump is mainly 3D physics in flow field [3-5]. So, 3D simulation of the centrifugal pump will give the clear information about the requirement of the modification in the impeller passage and blade geometry. In the flow passage of the centrifugal pump, fluid should flow in stream line with the blade geometry. However, flow separation, recirculation, reverse flow and vortex shedding in the flow passage would create the unfavourable noise in the pump during off-design condition. This noise from the centrifugal pump would help to predict the onset of cavitation [6]. The noise and vibration produced under the cavitating condition is used to measure its intensity and does not require any sensor to measure the level of cavitation [7]. Moreover, Zin *et al.*, [8] conducted experimental work to measure the FFT of the cavitation noise under the different operating condition like discharge, speed and corresponding vibration signal to correlate the cavitation noise and diagnosis the cavitation progressive in the pump. The numerical simulation has been performed by Park *et al* [9] to study the effect of Tip-vortex cavitation and its result on the change in nuclei size. Moreover, it is studied that the inception of cavitation and unsteady pressure is mainly influenced by the size of the bubble nuclei. It is observed that the bigger nuclei influence more on onset of cavitation and the smaller nuclei influence on the formation of the Tip-vortex cavitation. In the centrifugal pump, cavitation inception is observed at 3% head drop. As the continuous reduction of the net positive suction head of the centrifugal pump, the passage of the impeller identified as formation of the cavitation inception and the corresponding pressure drop would be the 3% [9]. The numerical analysis of centrifugal pump is not widely accepted as much as compared to the experimental results. However, it gives the reliable result at which direction to proceed further. Furthermore, it helps in predicting the performance of the pump at extreme off-design condition where practical experimentation is difficult to achieve. Based on the existing review of literature and practical experience in handling pump, the cavitation is the important parameter need to be consider for designing the centrifugal pump. The major other key design parameters are the clearance gap between the impeller and casing, chocking, etc. Pump Geometry. The centrifugal pump simulated in this work is the radial flow pump. The maximum vane outlet diameter of the pump is 358 mm and contains five backward curved blade. The meridional view of the centrifugal pump is shown in Fig.1, it shows that the eye radius of the impeller is r_1= 41mm and the outer radius of the impeller is r_2= 178mm. Figure 2 shows the development of the thickness of the blade from leading edge to trailing edge and its thickness is 5mm. The designed operating point of the pump is 20 lps discharge and head 40 m and it rotates at 1400 rpm. The blade angle at the inlet and outlet are β_1= 28° and β_2=35° respectively, and its wrap angle θ= 120°. Figure 4, shows the variation of θ and β from leading edge (LE) to trailing edge (TE) of the blade.

Manuscript published on 30 September 2019.
***Correspondence Author(s)**
Micha Premkumar T *, Department of Mechanical Engineering, Hindustan Institute of Technology and Science, Padur, India. Email: tmichamech@gmail.com
Sathish Babu R, Department of Mechanical Engineering, Hindustan Institute of Technology and Science, Padur, India.
Vinoth Kumar M, Department of Mechanical Engineering, Hindustan Institute of Technology and Science, Padur, India.
Hariram V, Department of Mechanical Engineering, Hindustan Institute of Technology and Science, Padur, India.
Seralathan S, Department of Mechanical Engineering, Hindustan Institute of Technology and Science, Padur, India.

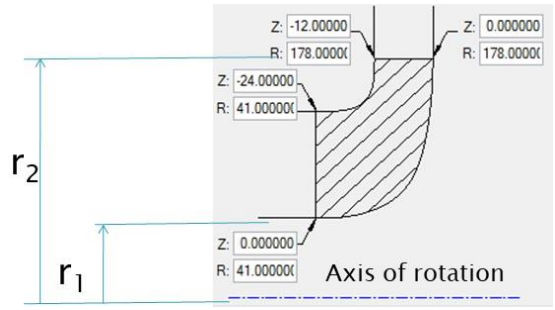

Fig. 1 Meridional view of the centrifugal pump

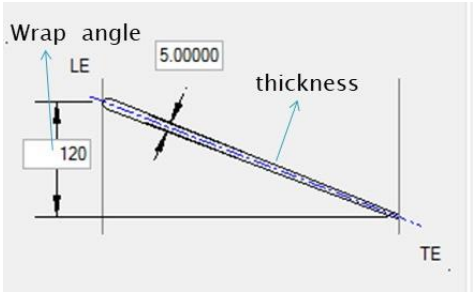

Fig. 2 Developed profile of the blade

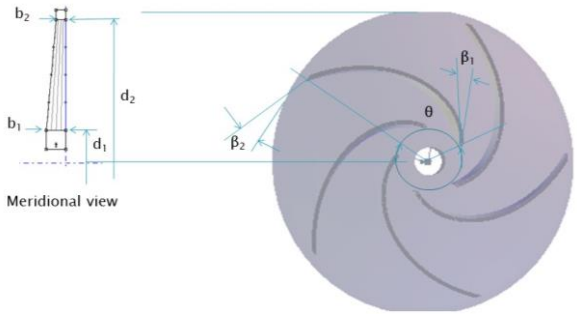

Fig.3 Schematic diagram of pump impeller with its meridional view.

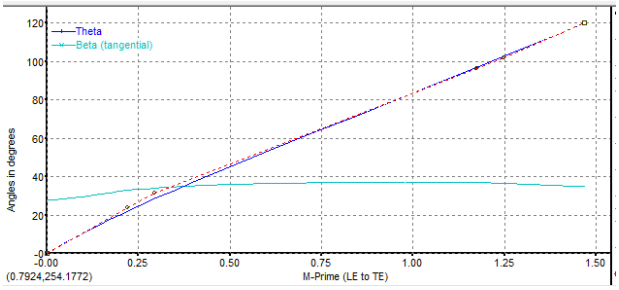

Fig.4 Variation blade angle from Leading edge to Trailing edge

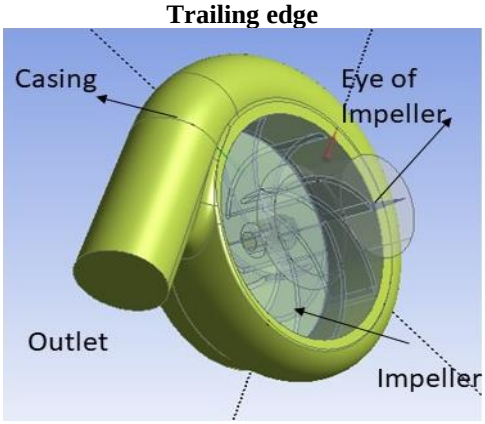

Fig.5 3D Model of the centrifugal pump

II. NUMERICAL METHODS

A. Grid Generation

Ansys© Turbo-grid© is used to generate grid for the impeller pump. Due to complexity in number of component in the pump impeller, careful examination of the grid in each component and proper distribution of the grid in the element is ensured. Unstructured hexahedral hybrid mesh is used everywhere in the component of the centrifugal pump. An extensive Grid sensitivity study was conducted for the element size ranging from 10000 to 50000 and the elements size of 20102 element per node per passage is sufficient to measure the pressure. So, total 1018015 element per node was used in this simulation for all passages. Total 152010 elements were used in the volute casing and 85031 were used in pump inlet region. Each model is carefully examined, refined and assembled step-by-step in order to get continuity between the components. The model gave confident, that in additional to the interaction between the flow of each component, the main fluid flow are effective modelled. Overall, 338842 element is used in this simulation and Fig.6a shows the total model mesh. Fig. 6b show the mesh in the flow passage and Fig. 6c shows the zoomed view of the leading edge of the blade, it shows that the O gird in the leading edge of the blade. The methodology is illustrated in a flow chart as shown in Figure 8.

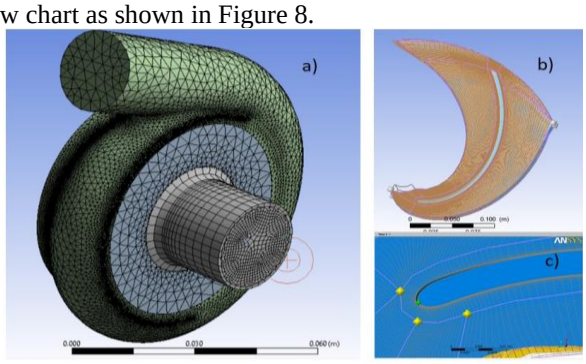

Fig.6 a) 3D Mesh of the complete centrifugal pump, b) Mesh in flow passage, c) zoomed view at the blade leading edge

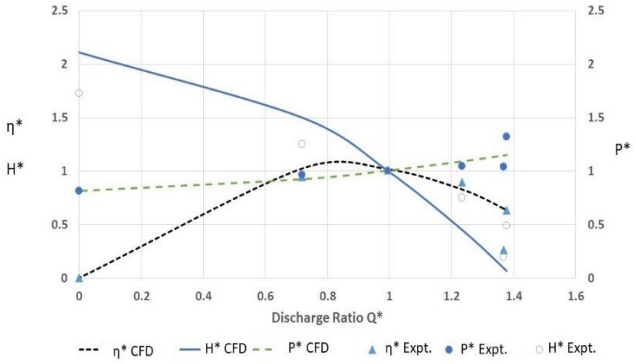

Fig.7 Comparison of Characteristics curve of Experimental Data with the numerical results

B. Pre-processing

The pre-processing of the numerical analysis of the centrifugal impeller is setup with transient analysis for entire set of the simulation.

Published By:
Blue Eyes Intelligence Engineering
and Sciences Publication (BEIESP)

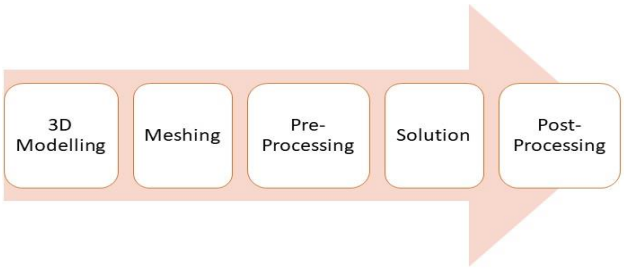

Fig. 8. Methodology of Numerical Simulation

The rotating reference frame method is used in the impeller. The general grid interference is used as the common reference between the stationary and rotating frame component. The mass flow rate is given as the inlet boundary condition and pressure outlet is given as the outlet condition. The internal and external surface of the impellers are modelled as the rotating wall and casing surface is modelled as the stationary wall. Second order unwinding discretization is employed for continuity and momentum equation. Turbulence model used is this simulation is the k-e RNG with cavitation model. In cavitation model, a homogeneous flow approach is employed. It is also called as Equal-Velocity-Equal temperature approach. The density of fluid is a function of vapour mass fraction *f*, which is calculated by solving a transport equation coupled with the mass and momentum conservation equations [12].

The $\rho - f$ relationship is

$$\frac{1}{\rho} = \frac{f}{\rho_v} + \frac{1-f}{\rho_l} \quad (1)$$

And the vapour volume fraction

$$\alpha = f\rho/\rho_v \quad (2)$$

The mass conservation equation for mixture

$$\frac{\partial}{\partial t}(\rho) + \nabla[(\rho\tilde{V}) = 0 \quad (3)$$

The momentum conservation equation for the mixture is

$$\frac{\partial}{\partial t}(\rho\tilde{V}) + \nabla[(\rho\tilde{V}\tilde{V}) = -\nabla_p + \nabla[[\mu_m(\nabla\tilde{V} + \nabla\tilde{V}^T)] \quad (4)$$

μ_m = Viscosity of mixture

$$\mu_m = (1-\alpha)\mu_1 + \alpha\mu_v \quad (5)$$

The vapour mass fraction f is governed by a transport equation

$$\frac{\partial}{\partial t}(\rho f) + \nabla[(\rho\tilde{V}_f) = \nabla[(\Gamma\tilde{V}_f) + R_e - R_c \quad (6)$$

R_c and R_e is the condensation and the evaporation rate, respectively, which is function of flow parameter like characteristic velocity, pressure, etc. , and fluid properties like liquid and vapour phase density, saturation pressure, and liquid and vapor surface tension.

When $p < p_v$

$$R_e = C_e\frac{\sqrt{k}}{\gamma}\rho_l\rho_v\sqrt{\frac{2(p_v-p}{3\rho_l}}(1-f_v-f_g) \quad (7)$$

And when $p > p_v$

$$R_c = C_c\frac{\sqrt{k}}{\gamma}\rho_l\rho_v\sqrt{\frac{2(p-p_v}{3\rho_l}}f_v) \quad (8)$$

where C_c and C_e are constant for empirical relation, k is the local kinetic energy, γ surface tension, f_v vapour mass fraction and f_v mass fraction of dissolved non condensable gases. The turbulence Model modelling was carried out using the standard $k-\varepsilon$ RNG model

The transport equation for standard $k-\varepsilon$ RNG model is

$$\frac{\partial}{\partial x_i}(\rho k u_i) = \frac{\partial}{\partial x_j}\left(\alpha_k\mu_{eff}\frac{\partial k}{\partial x_i}\right) + G_k - \rho\varepsilon \quad (9)$$

$$\frac{\partial}{\partial x_i}(\rho\varepsilon u_i) = \frac{\partial}{\partial x_j}\left(\alpha_\varepsilon\mu_{eff}\frac{\partial \varepsilon}{\partial x_j}\right) + C_{1\varepsilon}\frac{\varepsilon}{k}G_k - C_{2\varepsilon}\rho\frac{\varepsilon^2}{k} - C^*_{2\varepsilon}\rho\frac{\varepsilon^2}{k} \quad (10)$$

$$C^*_{2\varepsilon} = C_{2\varepsilon} + \frac{C_u\rho\eta^3[1-\frac{\eta}{\eta_o}}{1+\beta\eta^3} \quad (11)$$

G_k denotes the generation of turbulence kinetic energy due to the mean velocity gradients. α_ε and α_k are the inverse effective Prandtl numbers for ε and k, respectively. The RNG model is works well with rapid strain and streamlines curvature than the standard *k-ε* model. Delgosha *et al*. [11] suggested a modification to the standard *k-ε* RNG model, which reduced the mixture turbulent viscosity. In the standard *k-ε* RNG model, the turbulent viscosity is defined as

$$\mu_{eff} = \mu_t = \rho C_\mu\frac{k^2}{\varepsilon} \quad (12)$$

where $C_\mu = 0.0845$

The modified turbulent viscosity is defined as

$$\mu_t = f(\rho)C_\mu\frac{k^2}{\varepsilon} \quad (13)$$

where, n=10

III. RESULTS AND DISCUSSION

The pump model analysed in this work is low specific speed centrifugal impeller with head of 40m, discharge of 20 lps and speed of the impeller is 1440 rpm with specific speed of 12.8. The casing of the impeller is designed such a way that the uniform conversion of the kinetic energy into pressure energy is attained without any recirculation in the flow field to achieve the higher performance. The cautious in designing high performance centrifugal pump lies in the distribution of the blade angle along the meridional direction. The inlet blade angle of the impeller is arranged such a way that the inlet from the eye of the impeller matches with the inlet blade. Similarly, the outlet angle in the impeller blade is arranged to avoid swirl velocity at the exit. The variation of the blade angle between inlet and outlet is based on smooth distribution within the flow passage. Moreover, the flow inside the impeller is highly three dimensional due to vortices, return flow and other complex secondary flow and the blade angle distribution is shown in Fig.4. The performance test were conducted in the centrifugal pump at fixed rpm and for wide range of discharge. The experimental error for the various parameters were 1.3% for flow rate, 1% for total pressure and 1.5% for the shaft power at the design point. The experimental data is compared with the numerical results as shown in Fig. 7. Figure 9 (a, b) shows the stream line predicted with the numerical simulation at the off design discharge and it is observed that the vortex and the large separation is observed in the hub surface at 1.4 times the design discharge as seen in Fig. 9 (b). Figure 10 shows the velocity vector predicted using the CFD analysis and it shows the formation of the secondary flow pattern. Furthermore, the cross movement of the flow from the pressure surface of the blade to the suction surface is observed numerically in this analysis. It shows that the origin of the cross movement of the fluid is along the span wise direction along the blade suction blade surface.

Figure 11 shows the variation of the pressure contour at the mid cross section of the impeller, it shows that the low pressure field is formed in the front part of the suction surface of the blade and it is mainly due to the meridional secondary flow.

The total pressure loss is more in the corner of the blade due to the adverse pressure gradient and its less resistance to the downstream of the flow. Moreover, it is observed that the static pressure is not smooth at the entry of the blade, this is mainly due to the incompatibility of the Blade angle at the inlet. This can be avoided by redesigning the inlet blade angle. Fig. 12 (a) shows the variation of the volume fraction of the vapour fraction in the centrifugal pump. It shows that volume fraction 0 represent water and 1 represent vapour and Fig. 12 (b) show the contour of volume fraction of water present in the impeller passage.

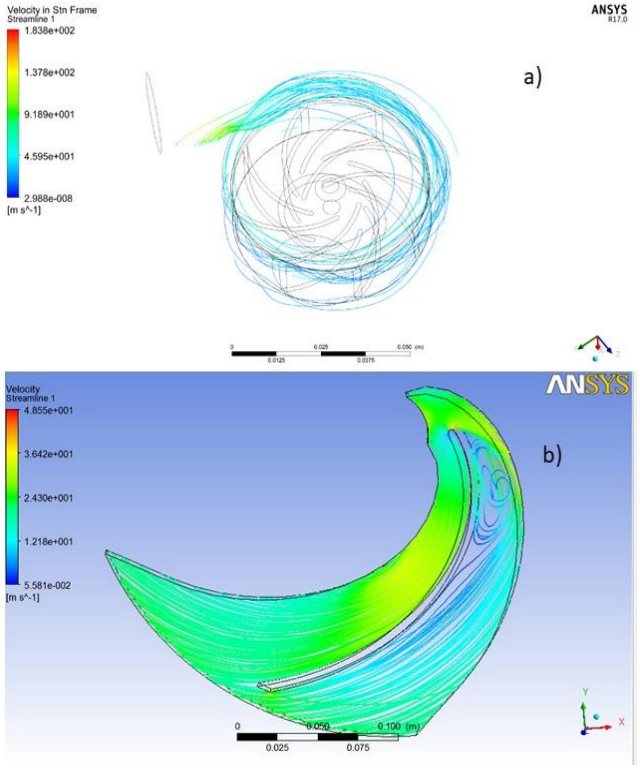

Fig 9. a) Stream line of the fluid flow inside the impeller, b) stream line in single passage of impeller

Table I. Experimental data of the centrifugal pump

Q*	H*	P*	η*
1.367087	0.197185	1.03816	0.263286
1.376522	0.488444	1.32104	0.630871
1.233478	0.754519	1.04952	0.899138
0.993913	1.005481	1.00416	1.009467
0.718043	1.256444	0.9664	0.946813
0	1.72963	0.8172	0

Table I gives the experimental data of the centrifugal pump non-dimensional with best efficiency points. Q*, H*, P* and η* are non-dimensional discharge, head, input power and efficiency respectively. The best efficiency point is identified from the Fig. 7 and these parameters are non-dimensionalised accordingly.

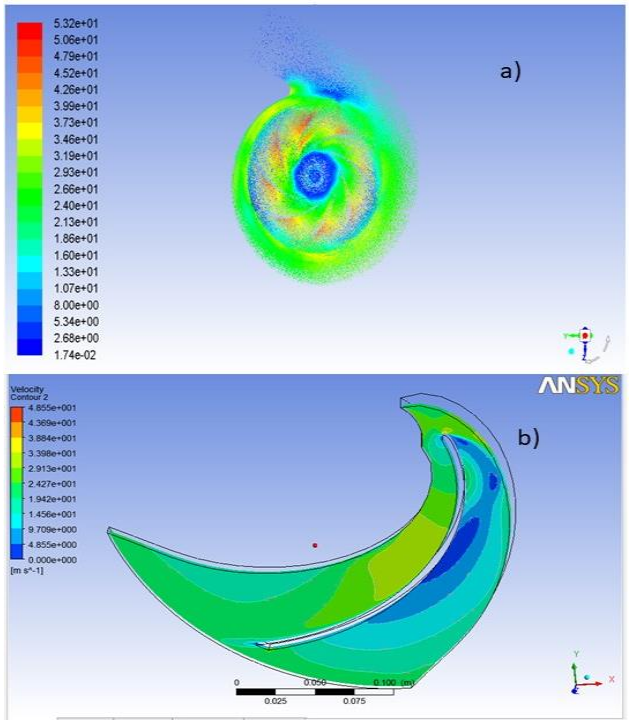

Fig.10 a) Velocity contour inside the impeller and b) velocity contour inside the single passage

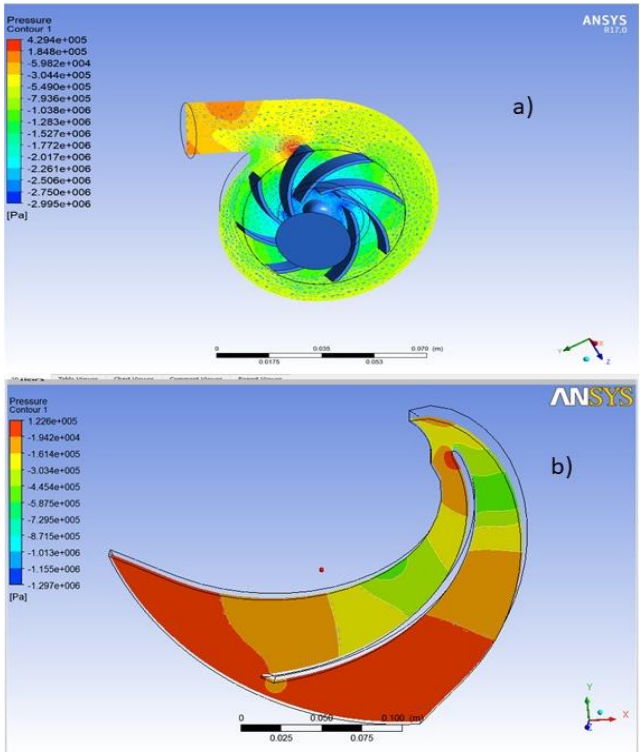

Fig.11 a) Pressure contour inside the impeller and b) Pressure contour inside the single passage

It shows that the volume fraction 0 represent water vapour and 1 represent water. It is observed from the figure that the upper surface the blade has cavitation, this is mainly due to presence of the recirculation and vortex in those region.

Retrieval Number: K21400981119/19©BEIESP
DOI: 10.35940/ijitee.K2140.0981119
Journal Website: www.ijitee.org

Published By:
Blue Eyes Intelligence Engineering and Sciences Publication (BEIESP)

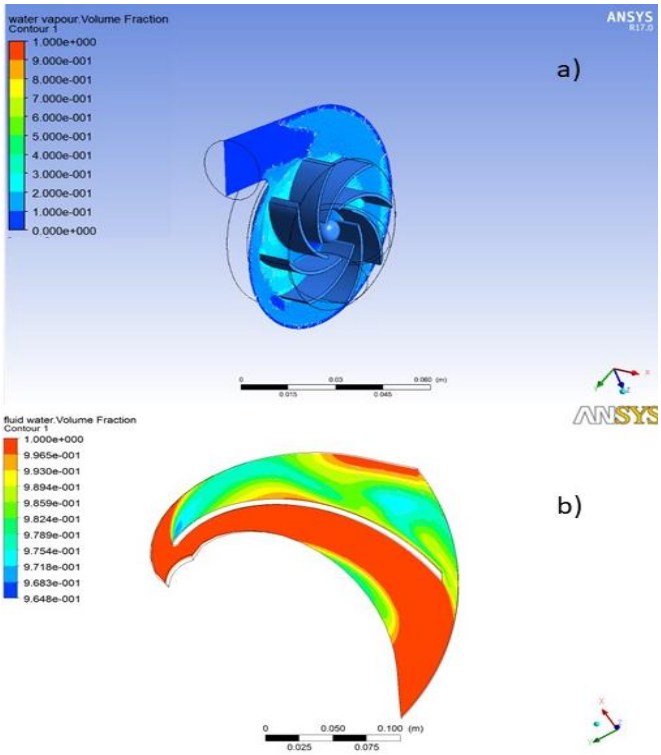

Fig. 12a) Contour of Volume fraction of the water vapour inside the impeller, volume fraction 0 in the contour scale represent water , b) Contour Volume fraction of water inside the blade passage, volume fraction 1 in the contour scale represent water

IV. CONCLUSION

The flow field analysis by CFD approach offers lot of opportunity to improve the hydrodynamic design of the centrifugal pump and other turbo-machines. However, the presence of the secondary flow, reversed flow, etc. in the flow passage would increase the complication in simulation due to those 3D effect. So, design and fine tune of the flow passage of centrifugal impeller is still crucial and it is mainly depends on the experience of the designer and past experimental data of the centrifugal pump. This paper is mainly based on the 3D design of the centrifugal pump and its passage, the validation of the numerical result is done by comparing with the experimental data. Moreover, the 3D CFD approach of centrifugal pump, extensively analysed the flow separation at the corner during the off-design working condition. This lead to formation of the cavitation in the centrifugal pump. This cavitation reduce the performance of the pump under off-design working condition. The validity of this methodology to measure 3D pressure field, velocity field and losses due to secondary flow has been established. Overall, appreciable development in analysing the hydraulic performance of the centrifugal pump is established by using the state-of-art CFD approach. Finally, in this work, the cavitation is observed in the leading edge of the suction surface in the impeller due to the separation and re-circulation at off-design condition (1.2 times of discharge).

REFERENCES

1. Sarath Kumar, R, T Micha Premkumar, S. Seralathan, T. Mohan, Numerical investigation of modified Bach type vertical axis wind turbine, Applied Mechanics and Material, 2016, 852, 551-557.
2. Saravanaa J Y, Rahul Kantamneni, Nizvan Fasil, Seralathan Sivamani, Hariram Venkatesan, Micha Premkumar T, Mohan T, "Modelling and analysis of water heating using recovered waste heat from hot flue gases of chulha", ARPN journal of engineering and applied sciences, 12(21), pp. 6164-6171, 2017.
3. Chaina Ram, Seralathan Sivamani, Micha Premkumar T, Hariram Venkatesan. "Computational study of leading edge jet impingement cooling with a conical converging hole for blade cooling", *ARPN journal of engineering and applied sciences*, 12 (22), pp. 6397-6406, 2017.
4. Lokesh Reddy B V, Yeswanth Yadav M, Micha Premkumar T, Seralathan S and Hariram V., " Modelling and Development of Passive Permanent Magnetic Bearing for a Small Cross Flow Vertical Axis Wind Turbine", *International Journal of Renewable Energy Research*, 8(4), pp. 1868 - 1880, 2018.
5. E. Kannan, Seralathan Sivamani, D G Roy Chowdhury, T Micha Premkumar, V Hariram. "Hole shape and influence of its orientation angle and arrangement on film cooling effectiveness", *Journal of Thermal Science and Engineering Application (ASME)*, 11(2), Article number 021014, 2019.
6. Cdina, M., 2003. Detection of cavitation phenomenon in a centrifugal pump using audible sound, Elsevier Science Ltd, 17(6): 1335-1347.
7. Parasuram, P.H. and G.P. Alexander, 2006. Sensorless detection of cavitation in centrifugal pumps, ASME International Mechanical Engineering Congress and Exposition, USA.
8. Zin, T.C., M.S. Leong and C. Lee, 2006. Field investigation of cavitation and flow induced vibrations in submerged vertical pumps in a power plant, Engineering Asset Management, pp: 1177-1186.
9. Park, K., H. Seol, W. Choi and S. Lee, 2009. Numerical prediction of tip vortex cavitation behaviour and noise considering nuclei size and distribution". Elsevier Ltd, Applied Acoustics, 70: 674-680.
10. Al-Arabi, A.B. and S.M.A. Selim, Saidur, R., Kazi, S. N., Duffy, G. G., 2011. Detection of Cavitation in Centrifugal Pumps, Australian Journal of Basic and Applied Science, 5(10): 1260-1267.
11. Coutier-Delgosha O, Fortes-Patella R, Reboud JL, et al. Experimental and numerical studies in a centrifugal pump with two-dimensional curved blades in cavitating condition. J Fluids Eng 2003;125(6):492–7.
12. ANSYS Fluent® Reference Manual, Release 12.0 ANSYS, Inc. 2009.